Liquid acoustic lens for photoacoustic tomography

Chaolong Song,† Lei Xi,† and Huabei Jiang*

Department of Biomedical Engineering, University of Florida, Gainesville, Florida 32611, USA
**Corresponding author: hjiang@bme.ufl.edu*

Received June 6, 2013; revised July 8, 2013; accepted July 14, 2013;
posted July 15, 2013 (Doc. ID 191854); published August 1, 2013

Recently, intensive research has been conducted to accelerate the development of photoacoustic (PA) imaging modality for biomedical applications. The use of acoustic lenses to collect ultrasound signals is of great interest. This Letter presents the design and fabrication of a liquid acoustic diverging lens, which can enlarge the acceptance angle of an ultrasound transducer. This lens possesses an inherent advantage of low acoustic impedance and the convenience to be attached to or detached from a commercial flat transducer. Phantom experiments have been carried out to demonstrate the improvement of using such a liquid lens over using a bare transducer for PA tomography.

OCIS codes: (110.5120) Photoacoutic imaging; (170.5120) Photoacoustic imaging; (170.6960) Tomography.
http://dx.doi.org/10.1364/OL.38.002930

Recently, there has been considerable interest in developing photoacoustic imaging (PAI) modality for biomedical diagnoses because PAI has the advantages of high optical contrast by optical illumination and relatively deep penetration by ultrasonic detection [1]. Generally, PAI falls into two categories: photoacoustic microscopy (PAM) and photoacoustic tomography (PAT) [2]. Acoustic lenses commonly present in both PAM and PAT systems can realize new functions or improve the imaging performance. Most acoustic-resolution PAM systems employ a focused transducer to collect the photoacoustic (PA) signal, which is inherently integrated with a converging (positive) lens [3–5]. Some optical-resolution PAM setups make use of the confocal concept in optics using a solid acoustic lens [6] or focused transducer [7] to align the ultrasound and illumination foci. Meanwhile, a diverging (negative) acoustic lens shows great capability to improve the performance of PAT by enlarging the acceptance angle. In this implementation, an acrylic plastic lens is glued on a flat transducer so that the directivity of the transducer is modified to cover a larger field of view (FOV). By adding the lens, the PAT system can reconstruct the image of a larger area with better accuracy [8,9].

Acoustic lenses have been demonstrated to be very helpful in PAI systems. They may play an equivalent role in ultrasound emission or detection as optical lenses in optical systems. However, light does not suffer from severe attenuation and reflection in most glass-based optical lenses, whereas the transmission efficiency of ultrasound in a solid-based acoustic lens is very low owning to the high acoustic impedance of a solid. Antireflection coating on the surface of a solid-based lens could increase the transmission [10], but the fabrication could be time consuming and not cost effective. Recently, the field of optofluidics has emerged to introduce the idea that solid-based optical components could be replaced by liquids or fluids with better performance and more functionality [11]. Since the acoustic impedance of liquid is much lower compared to a solid, building an acoustic lens with liquid can be advantageous. This Letter presents for the first time the design and fabrication of a liquid acoustic diverging lens for PAT. A hydrophone is used to map the pressure distribution of a transducer with and without the proposed liquid acoustic lens. Further experiments using the lens are carried out to demonstrate the advantages of such a lens in a PAT system.

Figure 1 shows the fabrication process of the liquid acoustic lens. A lens mold was physically built by a three-dimensional printer (Objet Eden 260V) from a predefined three-dimensional digital file [Fig. 1(a)]. Polydimethylsiloxane (PDMS) was mixed from two components (silicone elastomer base and its curing agent) with a weight ratio of 10:1. After the mixing and degassing, PDMS was poured into the mold and heated to 80°C for about 40 min [Fig. 1(b)]. When PDMS was cured after heating, it was peeled off from the mold and bonded with another piece of PDMS membrane [Fig. 1(c)]. The aperture of the lens was determined by the outer diameter of the transducer, which was 9.2 mm in this work. Liquid could be infused into the lens chamber by a syringe pump (KDS210, KD Scientific) through tubing and a needle [Fig. 1(d)]. The liquid lens as well as the transducer could

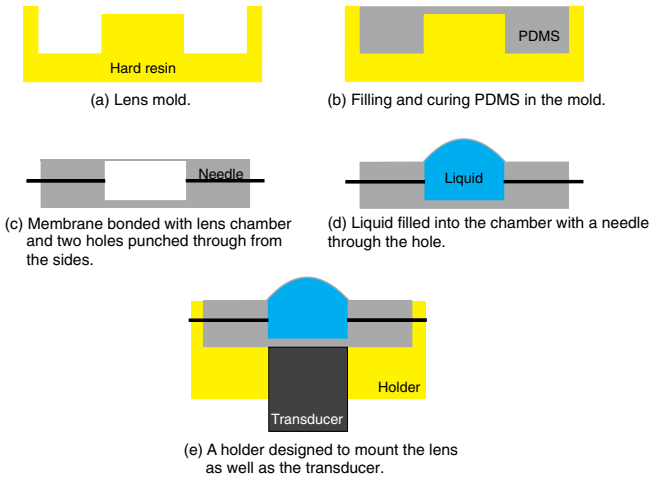

Fig. 1. Fabrication process. (a) Lens mold is built by a 3D printer, (b) PDMS is poured into the mold and cured at a temperature of 80°C, (c) piece of membrane (PDMS) is bonded and seals the lens chamber, (d) liquid is infused into the chamber through the holes to shape the curved lens interface, (e) holder, which is also made by a 3D printer, mounts the lens as well as the transducer.

be mounted on a holder (3D printer fabricated) with ultrasound gel in between [Fig. 1(e)]. Basically, the lens was formed by a pneumatic way, which has been reported for optical application [12] and micropump on a chip [13]. In this work, we purposely chose a glycerol (75%) and water (25%) mixture as the lensing liquid to apply this configuration for an acoustic application. The mixture had a density of 1.19 g/cm^3 and the speed of sound in this mixture was 1.78 mm/μs. The acoustic impedance of this mixture was 2.11 MRayl, which is lower compared to the impedance of aluminum 17.3 MRayl [10] and acrylic 3.23 MRayl [8,9].

In PAT, the acceptance angle of the transducer is a key factor that decides the accuracy of the image reconstruction. An ideal transducer for tomography should have a 360° acceptance angle to cover the whole FOV, but usually the directivity of a commercial flat transducer limits the acceptance angle. As a result of using a flat transducer, the reconstructed image may lose the true features of the targets, especially when the targets are located far from the center of the scanning area. Several works have been reported to enlarge the acceptance angle by gluing a diverging (negative) acrylic lens to a flat transducer [8,9]. However, problems associated with this method arise as follows: (1) the transducer can hardly be reused for other purposes because the removal of the acrylic lens may damage the transducer, and (2) the solid-based lens inherently has a high acoustic impedance, which leads to a considerable loss of the acoustic energy by reflection.

These problems motivated us to propose and test a liquid acoustic lens in this work. The testing of the lens was implemented in three steps: (1) the transducer worked in its transmission mode, and its pressure distributions with and without the liquid lens were mapped and compared; (2) pencil lead, as an ideal target, was used in PAT to look into how much image deformation would be caused due to the limited directivity for both cases with and without the lens; (3) a phantom was used to mimic tissue and was imaged by PAT for both cases with and without the lens.

In this test, the transducer (2.25 MHz, V133, Olympus) was in its transmission mode emitting ultrasound pulses. A holder mounted the transducer as well as the liquid acoustic lens and fixed their positions. A hydrophone (HNR-0500 ONDA) was employed to scan laterally and axially while detecting the ultrasound pulses from the transducer [Fig. 2(a)]. The signal was amplified and acquired by a computer. Figure 2(b) shows the pressure distribution of the transducer with and without the liquid lens. The peak to peak of the acoustic pressure is represented by the intensity value of each pixel, and all the values are normalized by the maximum value of the entire field. Without the lens, the bare transducer produced an acoustic beam covering a relatively smaller area of the field and it was slightly focused. On the other hand, the acoustic beam was expanded and covered a larger area by attaching the liquid acoustic lens to the transducer [Fig. 2(b)].

Seven pencil leads were aligned and embedded in a background with the rightmost one located at the center of the scanning area [Figs. 3(a) and 3(b)]. The background had an absorption coefficient of $\mu_a = 0.007$ mm^{-1} and a

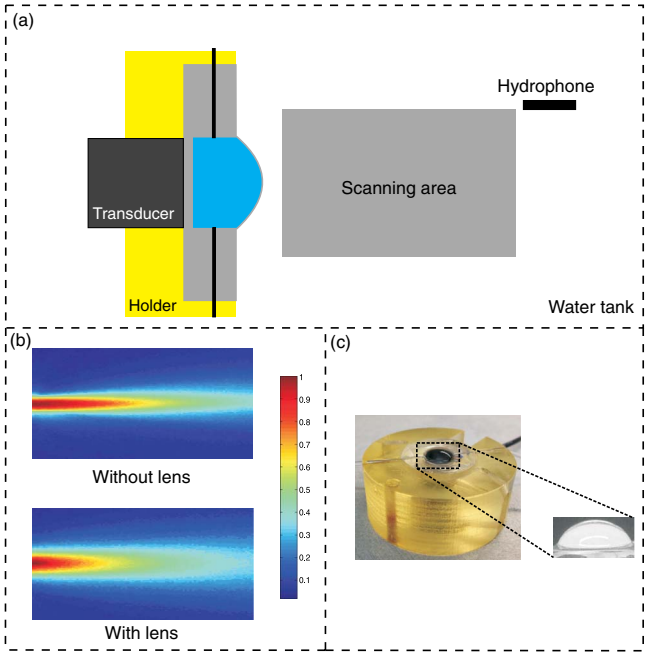

Fig. 2. (a) Schematic setup for testing the performance of the liquid lens, (b) acoustic pressure distribution of the transducer with and without the liquid lens, (c) photograph of the prototype of the liquid lens mounted on the holder.

scattering coefficient of $\mu_s = 1$ mm^{-1}. The absorption was introduced by adding ink. The experimental setup was the same as that used in the our previous work [14], except that the liquid acoustic lens was attached to the transducer in this experiment. A delay-and-sum algorithm was used to reconstruct the images [15].

Figures 3(a) and 3(b) show the comparison between the reconstructed images without and with the lens. In the absence of the lens, the image of the target started to suffer from tangential deformation when its distance from the center was about 5 mm. This effect of tangential deformation became increasingly magnified to the targets located farther from the center. The other observation was that the image contrast dropped with the increasing distance of the target from the center.

The tangential deformation was ubiquitously presented in PAI because the transducer was not an ideal point detector. Considering the circularly scanning detection method in most PAT systems, the effect of tangential deformation could be suppressed as long as the target could always be covered by the FOV of the detector. However, in reality, only the target close to the center could always be covered by the scanning detector. Therefore, the farther away the target was from the center, the worse its image deformation.

Enlarging the acceptance angle using a diverging lens is an efficient way to suppress the tangential deformation. Figure 3(b) shows that the image of the target (with black arrow pointed), located at about 15 mm away from the center, remained in an approximately similar shape as its true size. On the other hand, the corresponding image generated without the lens [Fig. 3(a)] went through a severe deformation. The tangential profiles of the images (with and without the lens) were plotted in Fig. 3(c). The comparison indicates that the diverging liquid acoustic

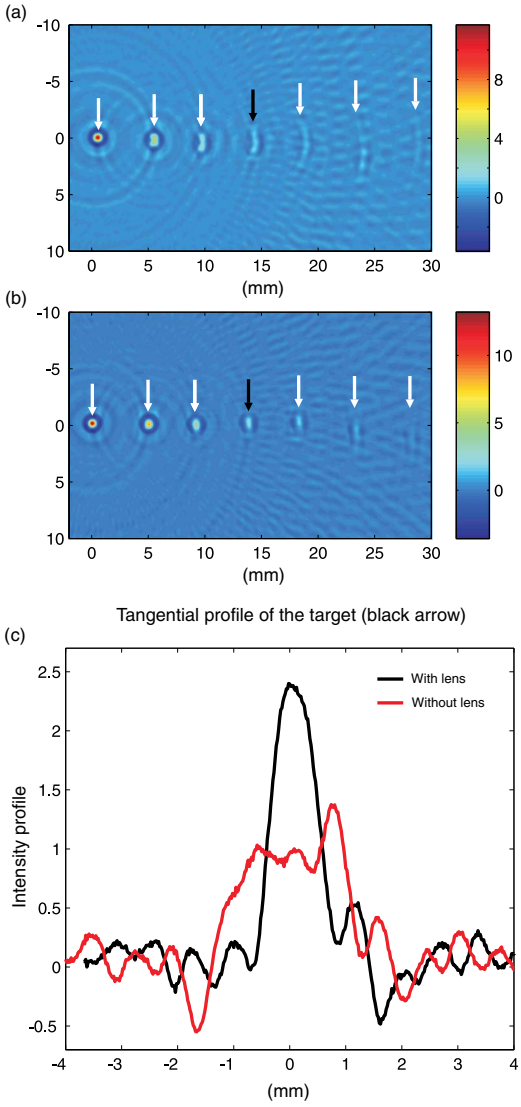

Fig. 3. PAT of pencil leads. Seven pencil leads (0.7 mm diameter) are aligned along the radial direction with the rightmost one located at the center of the scanning. (a) Imaging without liquid lens, (b) imaging with liquid lens, (c) intensity profile along the tangential direction of the pencil lead with black arrow pointed.

lens can efficiently suppress the deformation by enlarging the acceptance angle of the detector.

In the phantom experiments, three targets of the phantom, which had a $\mu_a = 0.049$ mm^{-1} and a $\mu_s = 0.1$ mm^{-1}, were positioned at the center (no. 1), with a horizontal distance of 11 mm from the center (no. 2), and with a vertical distance of 10 mm from the scanning plane (no. 3), respectively (Fig. 4). All the targets had the same diameter of 4 mm.

Figures 4(a) and 4(b) show the reconstructed images of PAT without and with the liquid acoustic lens, respectively. Generally, the image produced with the lens [Fig. 4(b)] had a better signal-to-noise ratio than that produced without the lens [Fig. 4(a)]. This is because the lens could enlarge the acceptance angle and cover a larger FOV, and thus the signals from the off-center targets could contribute more in the linear delay-and-sum reconstruction process.

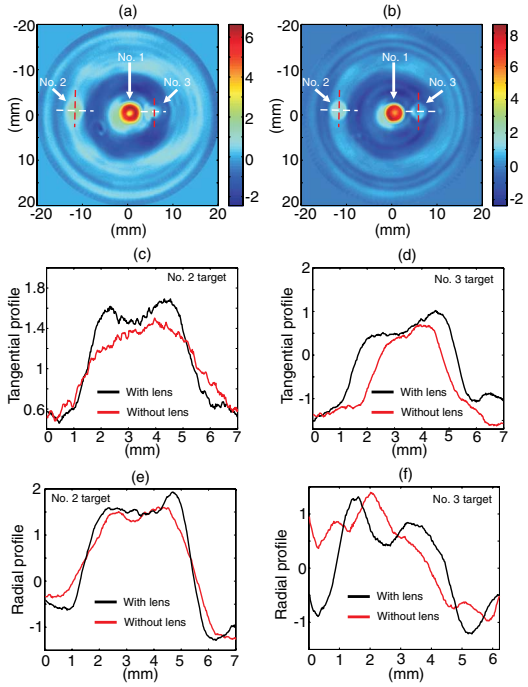

Fig. 4. Results of phantom experiments. A target (no. 1) is placed close to the center for reference. The no. 2 target is located in the same plane of no. 1 but with a distance of 11 mm from the center. The no. 3 target is lifted up to have a vertical distance of 10 mm from the center. All the targets have the same diameter of 4 mm. (a) Imaging without lens, (b) imaging with lens, (c) tangential profile of the no. 2 target, (d) tangential profile of the no. 3 target, (e) radial profile of the no. 2 target, (f) radial profile of the no. 3 target.

The no. 2 target located 11 mm away from the center was imaged to have tangential deformation without the lens. The comparison between the tangential profiles in Fig. 4(c) could apparently illustrate the deformation. On the other hand, the reconstruction of the image over the radial direction did not present any deformation under either condition with or without the lens [Fig. 4(e)].

Another interesting observation is the imaging of the target (no. 3) off the scanning plane. The image produced without using the lens presented only a fragment of the target, which was the part close to the central axis [Fig. 4(a)]. This is because the bare transducer with a limited directivity could only cover the signal emitted from the part of the target, which was close to the central axis of the scanning plane, and the signal of the other part, which was out of the detection cone of the transducer, could hardly be detected at any scanning points. This signal blind zone resulted in a phenomenon that was different from the tangential deformation of the no. 2 target. On the other hand, by enlarging the acceptance angle using the lens, the detection cone of the transducer could cover the entire body of the no. 3 target. As a result, the image could be correctly reconstructed [Fig. 4(b)]. Figures 4(d) and 4(f) show that the image produced with the lens remained approximately the true size of 4 mm diameter (tangential and radial), but the image produced without using the lens lost its fidelity by shrinking tangentially and distorting radially. Therefore, enlarging the detection cone using the liquid acoustic lens could also

be promising to improve the SNR and correct the imaging deformation in 3D PAT [16,17], which has been demonstrated as an effective imaging method for the diagnosis of breast cancer [18–20].

We have reported a liquid-based acoustic diverging lens for PAT. Compared to the previous solid-based acoustic lens, the liquid lens presented an inherently low acoustic impedance and a convenience to be attached to or detached from any commercial transducers without damaging the transducers, and the material PDMS that encapsulates the liquid is biocompatible, which makes this lens suitable for biomedical applications. Experiments were carried out to demonstrate the advantages of using such a liquid lens over using a bare transducer. The experimental results showed that the image of PAT can be reconstructed more accurately using the liquid diverging lens for both off-center and off-plane targets.

†Chaolong Song and Lei Xi contributed equally to this work.

References

1. V. Ntziachristos, Nat. Methods **7**, 603 (2010).
2. P. Beard, Interface Focus **1**, 602 (2011).
3. L. Xi, S. R. Grobmyer, G. Zhou, W. Qian, L. Yang, and H. Jiang, "Molecular photoacoustic tomography of breast cancer using receptor targeted magnetic iron oxide nanoparticles as contrast agents," J. Biophoton. (to be published).
4. L. Xi, L. Zhou, and H. Jiang, Appl. Phys. Lett. **101**, 013702 (2012).
5. X. Wang, D. L. Chamberland, and G. Xi, J. Neurosci. Methods **168**, 412 (2008).
6. K. Maslov, H. F. Zhang, S. Hu, and L. V. Wang, Opt. Lett. **33**, 929 (2008).
7. L.-D. Liao, M.-L. Li, H.-Y. Lai, Y.-Y. I. Shih, Y.-C. Lo, S. Tsang, P. C.-P. Chao, C.-T. Lin, F.-S. Jaw, and Y.-Y. Chen, NeuroImage **52**, 562 (2010).
8. W. Xia, D. Piras, M. Heijblom, J. C. G. v. Hespen, S. v. Veldhoven, C. Prins, W. Steenbergen, T. G. v. Leeuwen, and S. Manohar, in *Novel Biophotonic Techniques and Applications*, (Optical Society of America, 2011), p. 80900L.
9. C. Li, G. Ku, and L. V. Wang, Phys. Rev. E **78**, 021901 (2008).
10. J. J. Niederhauser, M. Jaeger, and M. Frenz, Appl. Phys. Lett. **85**, 846 (2004).
11. D. Psaltis, S. R. Quake, and C. Yang, Nature **442**, 381 (2006).
12. D. Y. Zhang, N. Justis, and Y. H. Lo, Appl. Phys. Lett. **84**, 4194 (2004).
13. H. Y. Tan, W. K. Loke, and N. T. Nguyen, Sens. Actuators B Chem. **151**, 133 (2010).
14. L. Xi, X. Li, and H. Jiang, Appl. Phys. Lett. **101**, 173702 (2012).
15. C. G. A. Hoelen and F. F. M. de Mul, Appl. Opt. **39**, 5872 (2000).
16. B. Wang, L. Xiang, M. S. Jiang, J. Yang, Q. Zhang, P. R. Carney, and H. Jiang, Biomed. Opt. Express **3**, 1427 (2012).
17. L. Xiang, B. Wang, L. Ji, and H. Jiang, Sci. Rep. **3** (2013).
18. L. Xi, X. Li, L. Yao, S. Grobmyer, and H. Jiang, Med. Phys. **39**, 2584 (2012).
19. S. Manohar, A. Kharine, J. C. G. van Hespen, W. Steenbergen, and T. G. van Leeuwen, J. Biomed. Opt. **9**, 1172 (2004).
20. S. A. Ermilov, T. Khamapirad, A. Conjusteau, M. H. Leonard, R. Lacewell, K. Mehta, T. Miller, and A. A. Oraevsky, J. Biomed. Opt. **14**, 024007 (2009).